

# Targeted Photodynamic Diagnosis of *In Vitro* Cultured Colorectal Cancer Cells

N W N Simelane, C A Kruger and H Abrahamse<sup>1</sup>

Laser Research Centre, Faculty of Health Sciences, University of Johannesburg, P.O. Box 17011, Doornfontein 2028, South Africa.

E-mail: cherier@uj.ac.za

**Abstract.** Colorectal cancer (CRC) currently remains a challenge to diagnose and is the third most diagnosed cancer worldwide. Photodynamic diagnosis (PDD) is a promising early diagnostic approach which uses photosensitizers for fluorescence detection of malignant cancer cells without inducing tumour damage. In this study, ZnPcS<sub>4</sub> a photosensitizer with pronounced chemical properties due to its tetra sulphonation was incorporated with specific CRC targeting antibodies (Anti-GCC Ab) on the surface of heterobifunctional aminefunctionalized and PEG stabilized gold nanoparticles (AuNPs), to form a final actively targeted PS nanoconjugate (ZnPcS<sub>4</sub> – AuNP-PEG5000-SH-NH<sub>2</sub> – Anti-GCC Ab). The final actively targeted PS nanoconjugate was successfully synthesized and characterized using spectroscopic techniques. Immunofluorescent photodiagnostic results confirmed that the final actively targeted PS nanoconjugate was able to localize within *in vitro* cultured CRC cells more specifically, due to its active targeting biomolecule (Anti-GCC Ab) than PS treatment alone. The final targeted PS nanoconjugate offered highly specific and sensitive absorption of the PS in CRC cells and so allowed for the successful photodynamic diagnosis of CRCs *in vitro*.

## 1. Introduction

Colorectal cancer (CRC) remains the fourth most commonly diagnosed cancer and represents about 9.4% of all estimated cancer deaths worldwide [1,2]. Additionally, CRC is the sixth leading cause of cancer death in South Africa [3]. Conventional CRC diagnostic techniques are often limited for early detection, as they lack specificity and are often invasive [4]. Moreover, the poor prognosis and decreased survival rate when CRC is identified at advanced stages raise a demand for an early diagnostic modality that can reduce cancer mortality [5].

Photodynamic diagnosis (PDD) is an emerging minimally invasive technique that may be utilized as an alternative option for the diagnosis of malignant disorders [6]. This technique offers advantages such as selective targeting and primary localized within tumor cells for specific identification [6]. The PDD technique relies on the combined use of an administered tumor targeted photosensitizer (PS), that when excited by blue light, emits a strong fluorescence signal that can be used to precisely diagnose cancer [5,7].

Zinc Phthalocyanine Tetrasulfonic acid (ZnPcS<sub>4</sub>) is a hydrophilic metallated PS that has been found to exhibit great potential in CRC photodynamic studies, due to its prolonged lifespan and passive absorption in tumor cells [8–10]. Since, ZnPcS<sub>4</sub> exhibits a characteristic short-blue B absorption band, between 330 to 350 nm, this particular PS could be possibly utilized within PDD applications [9].

Nanoparticles (NPs) are attractive carriers of PSs in PDD applications for improved diagnostic outcomes, since they enhance the PS accumulation in tumor cells via the enhanced permeability and retention effect (EPR), as well as can be further modified with specific tumor receptive site biomarker targets (such as antibodies), which promote actively precise PS absorption in marked tumors [11]. Gold nanoparticles (AuNPs) are the most promising PS carrier in photodynamic applications, since they have

---

<sup>1</sup> To whom any correspondence should be addressed.

a large surface area to accommodate high PS loading, as well as provide PS protection from biological barriers due to their immune biocompatibility [12]. Additionally, the large surface area of AuNPs accommodates further functionalization with various targeting moieties to deliberately enhance targeted active uptake and specific cellular localization of PSs for overall improved PDD outcomes [13].

Overall, the use of the active targeting approach that exploits the modification of NP-PS with celltargeting ligands, such as monoclonal antibodies (mAb) is a highly sought-after strategy in PDD applications, since it promotes PS internalization and accumulation and so enhanced specific and highly accurate cancer diagnosis outcomes [11]. The transmembrane receptor protein, guanylyl cyclase C (GCC) has been reported to be specifically overexpressed in CRC cells and so can be used as an active target biomarker within passive NP-PS conjugates to improve PS internalization for precise PDD [14].

Within this study, Anti-GCC monoclonal antibodies (mAbs) moieties were loaded onto AuNPs which were conjugated to ZnPcS<sub>4</sub> PSs, in order to construct a final targeted nanobioconjugate (BNC), that could possibly increase specific PS localization within in vitro cultured CRC and so enhance PDD precision.

## 2. Methodology

### 2.1. Chemical Synthesis and Molecular Characterization of the BNC

The final bionanoconjugate: ZnPcS<sub>4</sub> – AuNP-PEG5000-SH-NH<sub>2</sub> – Anti-GCC mAb (BNC) was synthesized according to Naidoo and co-workers [15]. Briefly, the ZnPcS<sub>4</sub> PS was conjugated onto the surface of AuNP-PEG5000-SH-NH<sub>2</sub> (Sigma-Aldrich: 765309), using spontaneous ligand exchange (between Au and PS tetra sulphides) and adsorption (disulphide bond between PEG and PS) techniques. 200µg/ml of Anti-GCC mAb (Abcam: ab122404) were activated using covalent mode carbodiimide crosslinker two-step coupling and bound to the surface of the already conjugated ZnPcS<sub>4</sub> PS - AuNP-PEG5000-SH-NH<sub>2</sub>, using EDC and NHS chemistry. The BNC was then subjected to UV Visible, DLS and ZP characterization, as well as immunofluorescent staining.

#### 2.1.1. UV-Visible Spectroscopy

The BNC contained ZnPcS<sub>4</sub> PS, which is known to absorb at 350nm (Soret Band) and emits at 583, 634 and 674nm (Q band) ranges in PBS [9]. The photostability of the BNC and its characteristic Soret and Q bands values were measured and confirmed using UV-Vis spectroscopy over the duration of experimental assays (8 weeks).

#### 2.1.2. Light Scattering (DLS) and Zeta potential

Particle size and zeta potential (ZP) of the BNC were measure by dynamic light scanning (DLS) on a Malvern Zetasizer Nano ZS (Malvern Instruments, Malvern UK), equipped with a 4mW He-Ne laser at a 633nm wavelength at 25°C, in triplicate, with all appropriate controls.

### 2.2. Cell Culture

Human colon cancer CaCo-2 (CaCo-2 Cellonex Cat SS1402) and normal human fibroblasts WS1 (ATTC CRL-1502) cell lines were cultured in DMEM Media or MEM media, respectfully, supplemented with 10% Foetal Bovine Serum (FBS), 4mM sodium pyruvate, 4mM L-glutamine, 2.5g/ml amphotericin B, and 100U Penicillin 100g/ml streptomycin solution. The cells were maintained in a humidified incubator with atmosphere of 5% CO<sub>2</sub> at 37°C. Upon confluency, the cells were harvested using TrypleSelect™ and seeded into a 3.4cm culture plates at a density of 6 x 10<sup>5</sup> cells, which contained a sterile coverslip. Culture plates were incubated for 4hrs to allow for cellular attachment.

### 2.3. Photo Diagnostic Assays

To determine if the BNC could be selectively absorbed by CRC cells only (and not by normal fibroblast cells), in order to be utilized as a fluorescent marker for the early CRC PDD, intercellular cell adhesion

molecule-1 (ICAM-1) immunofluorescent membrane staining and fluorescent microscopy imaging assays were performed. Post 4hrs attachment culture plates received a predetermined effective dose of  $0.125\mu\text{M}$  ZnPcS<sub>4</sub> PS only, ZnPcS<sub>4</sub> – AuNP-PEG5000-SH-NH<sub>2</sub> and BNC in 3ml of supplemented culture media to form various control and experimental groups. The culture plates were then incubated in the dark at 37°C overnight. Thereafter, the cells in the culture plates were rinsed using PBS and fixed with 3.7% paraformaldehyde for 10min at room temperature. The cells were then incubated with 2 $\mu\text{g}/\text{ml}$  ICAM-1 mouse monoclonal IgG1 (AbAB2213 AC: Abcam) and 5 $\mu\text{g}/\text{ml}$  Goat anti-mouse IgG-FITC (AB6785 AC: Abcam) on ice, for 30min at room temperature. After incubation, the cells were rinsed with HBSS, and the coverslips were mounted into microscope slides. Immuno fluorescent microscopic images were captured with a Carl Zeiss Axio Z1 Observer with FITC green (cell membranes) and DAPI blue (ZnPcS<sub>4</sub> PS) detection filter fluorescent settings, at 400x magnification.

### 3. Results

#### 3.1. Molecular Characterization of the BNC

##### 3.1.1. UV-Visible Spectroscopy

The UV-vis spectra of the BNC, noted no significant changes or deformations over an 8 week period, suggesting that it remained photostable (Figure 1). Additionally, the 340nm Soret band for the ZnPcS<sub>4</sub> PS within the final BNC remained high and prominent suggesting it conserved its photochemical properties, without any quenching and so could be utilized within PDD CRC *in vitro* assays fairly successfully.

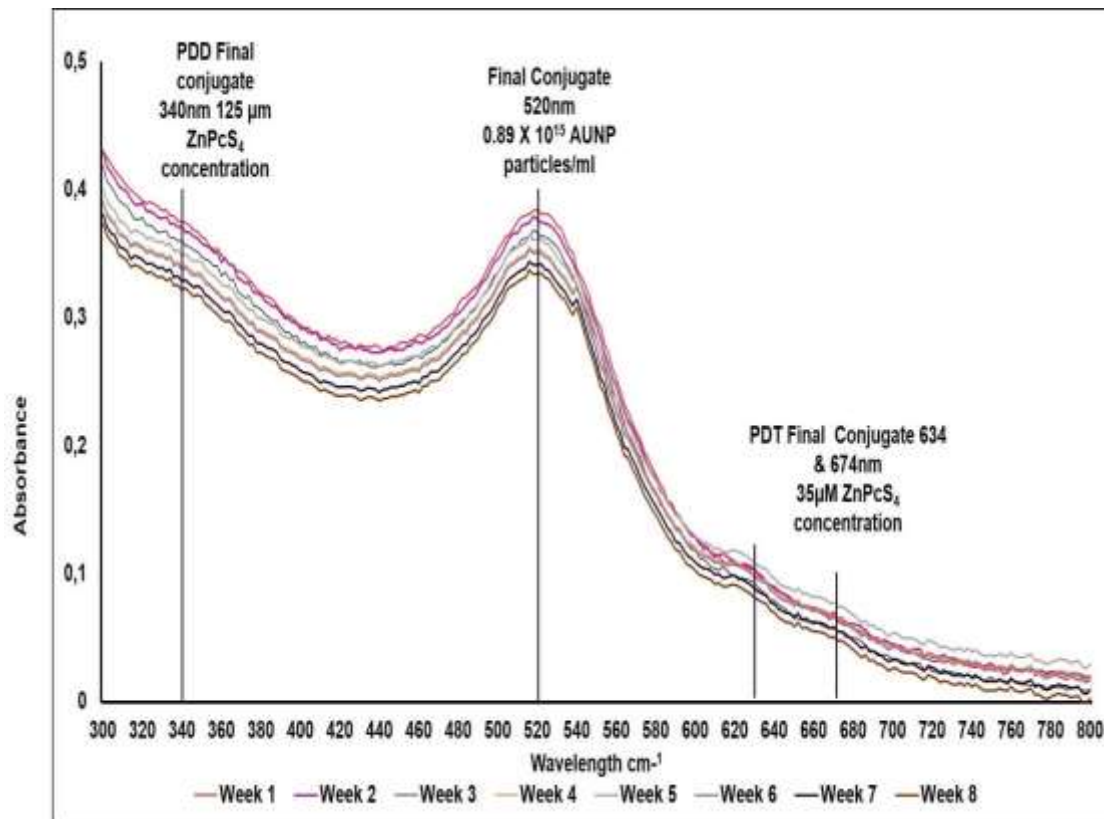


**Figure 1.** UV-vis spectroscopy measurements. Absorption spectra with respect to the ZnPcS<sub>4</sub> PS contained within the final BNC.

### 3.1.2. Dynamic Light Scattering (DLS) and Zeta Potential (ZP)

Within dynamic light scattering studies, the BNC reported one single major peak with a narrow width and no additional smaller side peaks, when repeated in triplicate (Figure 2). These findings demonstrated that a components of the final BNC were successfully bound [16]. Additionally, the DLS Polydispersity Index (PDI) value of the final BNC was found to be 0.353, reporting that it was a single monodisperse homogenously pure molecule, that had no aggregation. ZP results reported the BNC had a mean hydrodynamic diameter of  $57.18 \pm 3.04$  nm, suggesting it was small enough for cellular absorption [17]. The final BNC had a ZP value  $36.5 \pm 2.6$  mV, noting it was highly stable with a slight positively charge and should so would remain intact within an *in vivo* environment, as well as be retained more selectively by tumour cells which are negatively charged [16,18].

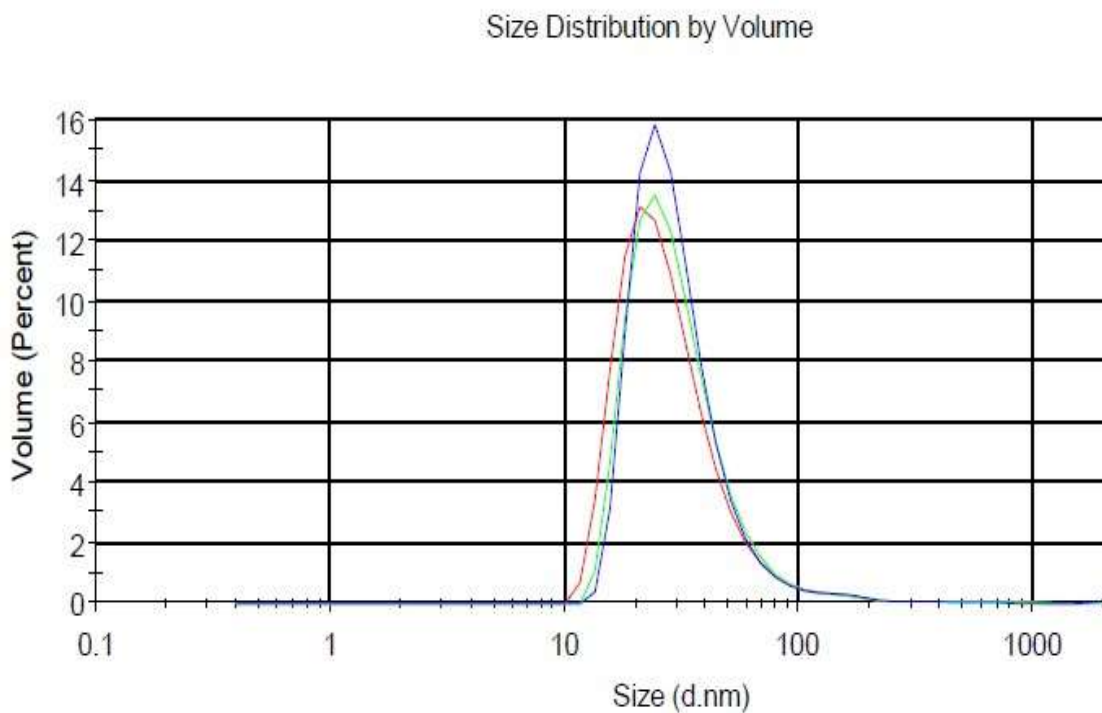


**Figure 2.** DLS hydrodynamic radius distribution graph of the final BNC.

### 3.2. Photo Diagnostic Assays

Fluorescent microscopy imaging was performed within various control and experimental groups to confirm the specific and targeted ZnPcS<sub>4</sub> PS absorption within CRC Caco-2 versus normal WS1 human fibroblast cells. Green immunofluorescent ICAM-1 / FITC membrane staining and ZnPcS<sub>4</sub> PS blue 340 nm fluorescence signals from the images were captured and examined. With reference to the first row of CRC images in Figure 3, the blue fluorescence intensity of ZnPcS<sub>4</sub> PS was far higher within the BNC experimental group than when compared to the other control groups. The control group of ZnPcS<sub>4</sub> PS alone reported less blue fluorescence intensity in CRC cells than when compared to the control group which received AuNP-PEG5000-SH-NH<sub>2</sub> - ZnPcS<sub>4</sub>. These observations suggest that the AuNPs were responsible for improved passive localization of the PS in CRC cells than compared to when it is administered in singular form [19]. Nevertheless, the CRC experimental group which received the final BNC, noted the highest blue fluorescence intensity, suggesting the most significant uptake of ZnPcS<sub>4</sub>.

PS was found. These observations suggest that the conjugated Anti-GCC mAbs, within the final BNC, successfully facilitated an active up-take of the PS, directed towards GCC overexpressed cellular surface receptors and so a far higher retention of the PS was found [14,20). With reference to the second row of WS1 normal human fibroblast images in Figure 3, the experimental cells which received the final BNC showed no selective or active accumulation retention of the blue stained ZnPcS<sub>4</sub> PS, in comparison to the control groups which received ZnPcS<sub>4</sub> PS alone or AuNP-PEG5000-SH-NH<sub>2</sub> - ZnPcS<sub>4</sub>.

These observations suggest that the final BNC had no specific targeting affinity for normal human cells and so could be successfully utilized in PDD application to distinguish between normal and in vitro cultured CaCo-2 CRC cells, however if ZnPcS<sub>4</sub> PS was to be administered alone or in conjugation with AuNPs its cellular uptake would not be specific enough to differentiate between in vitro normal and CRC cultured cells.

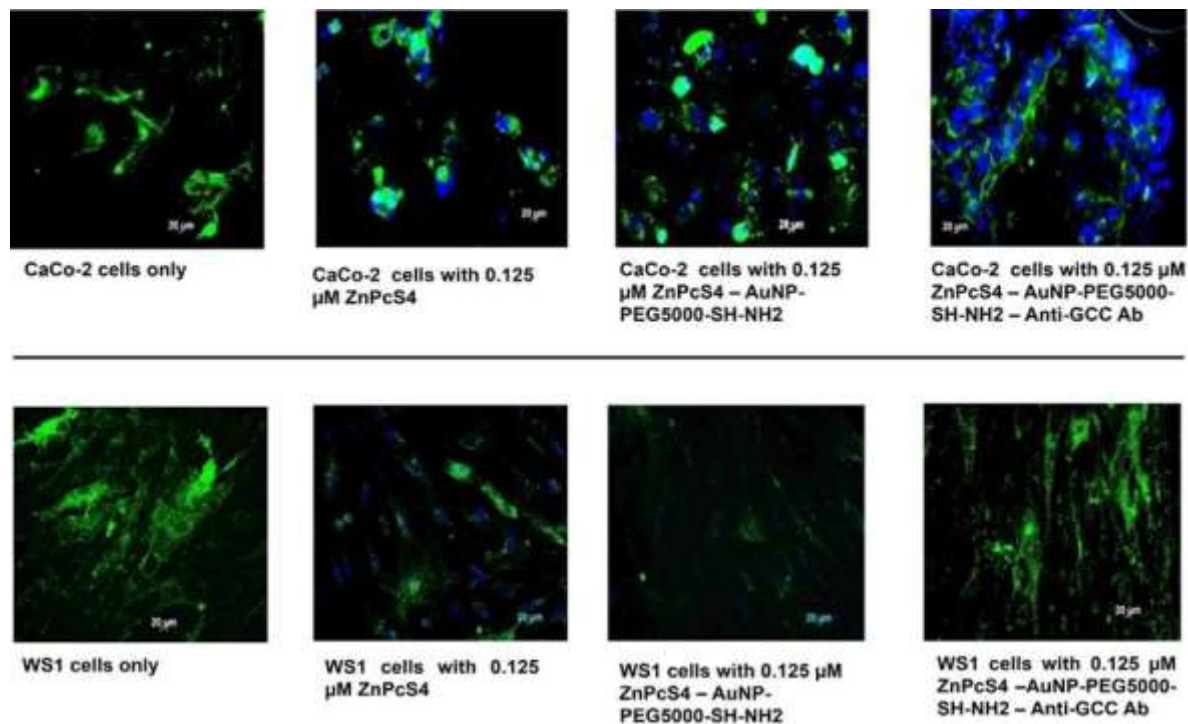


**Figure 3.** PDD fluorescent microscopy images comparison of ZnPcS<sub>4</sub> PS uptake in CRC CaCo-2 versus normal WS1 fibroblast cells, treated with ZnPcS<sub>4</sub> PS alone, AuNP-PEG5000-SH-NH<sub>2</sub> - ZnPcS<sub>4</sub>, and the final BNC. Cellular ICAM membrane proteins (GREEN stain), and ZnPcS<sub>4</sub> PS localization (BLUE stain).

#### 4. Conclusion

In conclusion, a novel final BNC, consisting of ZnPcS<sub>4</sub> PS with CRC specific targeting Anti-GCC mAbs conjugated to PEGlated AuNP was successfully synthesized. Molecular characterization assays confirmed that all components within the final BNC were successfully bound and that it displayed its signature Soret ZnPcS<sub>4</sub> PS PDD band at 340 nm. DLS and ZP results reported the final BNC was stable, monodisperse and of an acceptable size for cellular nano-targeting. Control groups which consisted of ZnPcS<sub>4</sub> PS bound to AuNP-PEG5000-SH-NH<sub>2</sub>, did note an improved passive uptake of the PS for PDD in CRC, however owing to the attachment of the Anti-GCC mAbs within the final BNC, it reported a highly active, localized, and enhanced uptake of the ZnPcS<sub>4</sub> PS and so was capable of the specific and

targeted PDD identification of CRC, since it showed no affinity for normal human WS1 fibroblast cells. Overall, this study demonstrated that the final BNC could be a promising platform for early targeted photodynamic diagnosis of CRC and so requires *in vivo* investigation.

## 5. Acknowledgements

This work is based on the research supported by the South African Research Chairs Initiative of the Department of Science and Technology and National Research Foundation of South Africa (Grant No 98337), Cancer Association of South Africa (CANSA) Research Funding Grant and National Research Foundation Thuthuka Fund (Grant No TTK180409318735).

## 6. References

- [1] Rawla P, Sunkara T and Barsouk A 2019 *Prz Gastroenterol.* **14** 89–103
- [2] Sung H, Ferlay J, Siegel RL, Laversanne M, Soerjomataram I, Jemal A and Bray F 2021 *CA: Cancer J. Clin.* **71** 209-49
- [3] Brand M, Gaylard P and Ramos J 2018. *SAMJ.* **108** 118-22
- [4] Naidoo C, Kruger CA and Abrahamse H 2019 *Molecules* **24** 3153
- [5] Simelane NWN, Kruger CA and Abrahamse H 2020. *RSC Adv.* **10** 41560-76
- [6] Agostinis P, Berg K, Cengel KA, Foster TH, Girotti AW, Gollnick SO, Hahn SM, Hamblin MR, Juzeniene A, Kessel and D, Korbek M 2011 *CA: Cancer J. Clin.* **61** 250-81
- [7] dos Santos AF, de Almeida DR, Terra LF, Baptista MS and Labriola L 2019 *JCMT* **5**
- [8] Nombona N, Maduray K, Antunes E, Karsten A and Nyokong T 2012 *J Photochem Photobiol* **107** 35-44
- [9] Brozek-Pluska B, Orlikowski M, Abramczyk H, Kadish KM, Smith KM and Guillard R 2016 *Handbook of Porphyrin Science* **36** 1-49
- [10] Brozek-Pluska B, Jarota A, Kania R and Abramczyk H 2020 *Molecules* **25** 2688
- [11] Kruger CA and Abrahamse H 2018 *Molecules* **23** 2628
- [12] Dube E and Nyokong T 2019 *J. Lumin* **205** 532-9
- [13] Calavia PG, Bruce G, Pérez-García L and Russell DA 2018 *Photochem. Photobiol. Sci.* **17** 153452
- [14] Danaee H, Kalebic T, Wyant T, Fassan M, Mescoli C, Gao F, Trepicchio WL and Rugge M 2017 *PLoS One* **12** e0189953
- [15] Naidoo C, Kruger CA and Abrahamse H 2019 *Oncotarget* **10** 6079
- [16] Patel VR and Agrawal YK 2011 *J. Adv. Pharm. Technol. Res* **2** 81–7
- [17] Yu X, Trase I, Ren M, Duval K, Guo X and Chen Z 2016 *J. Nanomater* **2016**
- [18] Bhattacharjee S 2016 *J. Control. Release* **235** 337-51
- [19] Hong EJ, Choi DG and Shim MS 2016 *Acta Pharm. Sin. B.* **6** 297-307
- [20] Hodgkinson N, Kruger CA and Abrahamse H 2017 *Tumor Biol.* **10** 1010428317734691.